International Journal of Mining and Geo-Engineering

IJMGE

IJMGE 53-2 (2019) 117-121

DOI: 10.22059/ijmge.2019.264023.594755

Effect of ventilation air velocities on diesel particulate matter dispersion in underground coal mines

Ramakrishna Morla [a, *], Shivakumar Karekal [a], Ajit Godbole [a], Ram Madhab Bhattacharjee [b], Nasina Balasubrahmanyam [c] , Inumula Satyanarayana [c]

[a] *School of Civil, Mining and Environmental Engineering, University of Wollongong, Australia*

[b] *Department of Mining Engineering, Indian Institute of Technology (ISM), Dhanbad, India*

[c] *Directorate General of Mine Safety (DGMS), India*

Article History:

Received: 19 August 2018,

Revised: 20 December 2018

Accepted: 01 January 2019.

ABSTRACT

This paper presents a detailed account of computational fluid dynamics (CFD) simulations undertaken to investigate the influence of intake (ventilation) air velocities on the flow patterns of diesel particulate matter (DPM) generated by a man-riding vehicle operating in a straight rectangular cross section tunnel in an underground coal mine. The simulation results are validated against an earlier experimental study. At a sampling station 10 m downstream of the vehicle, the DPM concentration was seen to decrease rapidly with increasing intake air velocity. For air velocities of 0.5 m/s, 1 m/s, 2 m/s and 3 m/s, the DPM concentration was estimated to be 233 µg/m^3, 131 µg/m^3, 116 µg/m^3 and 1 µg/m^3 respectively. At 10 m downstream of the vehicle, if the intake air velocity is reduced from a base value of 1.26 m/s by 40% and 60% of the base value, the average DPM concentration increased to 58% and 123% respectively. If the intake air velocity is increased by 58% and 98% of the base case value, the average DPM concentration decreased to 44% and 78% respectively.

Keywords : *Coal mines; DPM; Health effects, Air velocity; CFD; Man-riding vehicle*

1. Introduction

Diesel-operated man-riding vehicles are used to carry workers from the portal to specific sites in underground mines. These vehicles minimize the coal mine operators' travel time and thus improve their performance and efficiency. A number of mines have been using these vehicles [4]. However, the main drawback with these vehicles is their exhaust fumes, which contain diesel particulate matter (DPM) and other pollutant gases [5].

The chemical composition of DPM depends on the composition of the fuel and the lubricating oil, engine technology, operating conditions, and the technology used to treat the exhaust [2]. The major contributors to the total particle mass emitted by diesel engines include elemental carbon (EC), organic carbon (OC), inorganic compounds such as sulphates, nitrates, ammonia, sodium, chloride ions, and trace metallic compounds [1]. EC and OC emissions, cumulatively known as 'total carbon' (TC), make up the largest fraction of aerosols emitted by diesel engines, about 70% to 90% of DPM. On an average, EC comprises 50% to 70% of TC and greater than 45% of the total engine DPM emissions [1]. In this paper it is assumed that DPM is made up of EC only.

Various research studies have been conducted to better understand the effects of DPM on human health (e.g. [5, 7-9, 19-21]). These studies have concluded that exposure to diesel exhaust (or diesel particulates) for a substantial period of time may cause cancer in humans.

As per the Australian mine's regulations [3, 5, 17-18], the recommended safe 8-hour time-weighted average exposure standard of EC expelled from a diesel engine is 100 µg/m^3. This corresponds approximately to 160 µg/m^3 TC or 200 µg/m^3 DPM. As per mine regulations [3, 5, 17-18], it is recommended that the minimum ventilation required to minimize the health hazards due to diesel emissions and heat stress in places where a diesel engine operates shall be such that a ventilation air current of at least 0.06 m^3/s/kW corresponding to the maximum capacity (kW) of the engine, or 3.5 m^3/s, whichever is greater. If more than one diesel engine is being operated in the same ventilation current, it is recommended that the cumulative diesel engine rating (kW) shall be considered in the estimate [5].

Mapping of DPM flow patterns is required to develop effective DPM dispersion control strategies and to minimize exposure to personnel. This paper presents an analysis of the effect of ventilation air currents on DPM flow patterns near a diesel-powered man-riding vehicle located in a mine tunnel. The analysis is carried out using CFD simulations that are validated against field experimental data. Field experiments have been conducted near a stationary vehicle located in a working section of an underground coal mine.

2. Experimental Investigation

To monitor DPM concentration near a man-riding vehicle, field experiments were conducted in one of the eight working seams of an Indian coal mine [6]. To ensure that the intake air was free of DPM, the experiment was conducted in an isolated intake airway (mine gallery). The average width and height of the mine gallery were 6 m and 2.7 m respectively. To monitor DPM concentration, an 'Airtec' real time DPM monitoring instrument was used [16]. During the experiment, the flow rate of the DPM was adjusted to 2.83 x 10^{-5} m^3/s (1.7 liters per minute).

During field experiments, three sampling stations located at 1 m, 5 m and 10 m from the vehicle were selected. Each station had three

* Corresponding author. *E-mail address:* ramsiit99@gmail.com (R. Morla).

sampling points at a height of 1. 2 m from the floor. Fig. 1 shows the locations and arrangements of sampling stations and sampling points (a, b and c) on the downstream side of the man-riding vehicle. During the experiments, the average velocity of the air flow was maintained at 1.26 m/s. To ensure that the intake air was devoid of DPM, the experiment was conducted in one of the main intakes which passes from surface to the mine working section. The velocity of the DPM-carrying smoke was measured with a digital anemometer and was found to be 29 m/s. The temperature of the exhaust smoke was measured with thermocouple digital thermometer, and was found to be 323 K.

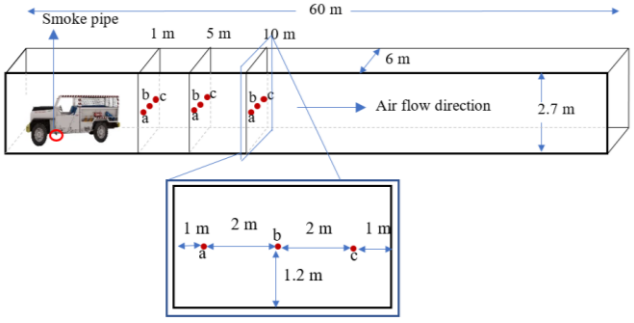

Fig. 1. Locations of sampling stations and sampling points with respect to DPM source.

3. CFD modelling

The computational domain in the CFD simulations corresponds to the 60 m long, rectangular cross section gallery in which the experiments were conducted. The shape of the man-riding vehicle was designed using AutoCad and imported into the computational domain. The length, width and height of the man-riding were 6.25 m, 2 m, 1.95 m respectively [6]. The location of the smoke pipe is behind the left front wheel and on the opposite side of the vehicle operator. The engine was equipped with a diesel particulate filter and the exhaust flow is a mixture of DPM and air. Fig. 2 shows the details of the constructed CFD model. Fig. 3 shows the details of meshed man-riding vehicle (a) and man-riding vehicle with gallery (b). To achieve accurate results, finer mesh was used with half-million computational cells. The minimum size of the cells was $7.3x10^{-3}$ m, minimum edge length of cells was 0.025 m and size function was proximity and curvature. Program controlled inflation with seven layers were used for the mesh. For this investigation, DPM is treated as a gas and chemical reactions were not considered. The flow in the domain was considered as Boussinesq approximation and turbulent.

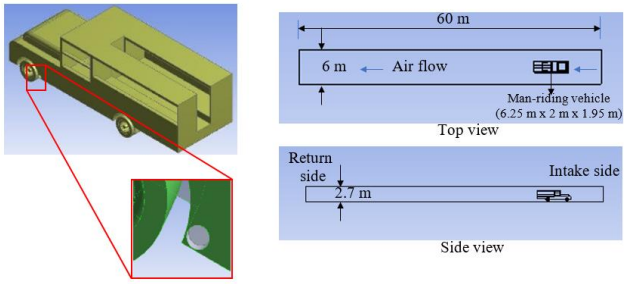

a. CAD model of man-riding vehicle with detail showing location of exhaust port

b. Computational domain used in the CFD model

Fig. 2. CFD model of man-riding vehicle and experimental gallery.

4. 'Base case' DPM dispersion model validation

DPM-related CFD modeling studies have been conducted in metal/non-metal mines using 30 kW stir skid loaders [10-14] and in coal mines with man-riding vehicles [6, 15]. The 'base case' CFD simulations were conducted with 1.26 m/s intake air velocity, identical to that used in the coal mine where the experiments were conducted. Fig. 4 show the base case CFD modelling results of DPM concentration at 1m, 5 m and 10 m downstream to the vehicle [6]. Table 1 compares the results of the base case simulations and field experiments at 1 m, 5 m and 10 m downstream of the vehicle and at the sample points 'a', 'b' and 'c'. The simulation results are in fair agreement with the experimental measurements at the three sampling stations. The slight discrepancies can be due to the roughness of the gallery wall surface, which was not considered in the CFD model. Despite simplifying assumptions in the simulations, the difference between simulation results and experimental measurements varies from -14.2% to + 14%.

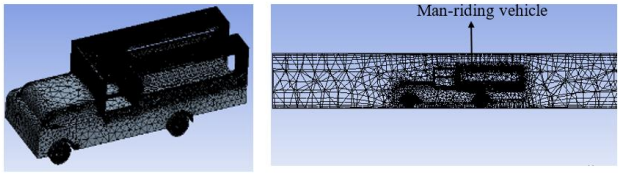

a. Surface mesh for man-riding vehicle

b. 3D mesh of gallery (airway)

Fig. 3. (a) Surface mesh for the vehicle, and (b) mesh for the airway.

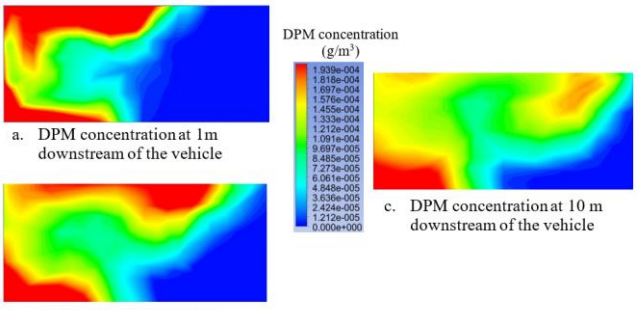

a. DPM concentration at 1m downstream of the vehicle

b. DPM concentration at 5m downstream of the vehicle

c. DPM concentration at 10 m downstream of the vehicle

Fig. 4. DPM concentration at 1 m, 5 m and 10 m downstream of the vehicle.

Table 1. Comparison of simulated DPM results with experimental results.

Sampling point	Experimental value (µg/m³)	Simulation value (µg/m³)	Difference %
	At sample station 1 m		
a	185.8	176	- 5.2
b	50	46	-8.0
c	0	0	0
	At sample station 5 m		
a	149.0	130	-12.7
b	117	110	-5.9
c	16	16	0
	At sample station 10 m		
a	127.4	130	2.0
b	116.6	100	-14.2
c	50.0	57	14.0

Note: difference % is the difference between simulation results and test results and is calculated as (simulation value– Experimental value)/ experimental value) × 100%.

5. Results and discussion

To understand the effect of intake air velocity of DPM dispersion, simulation studies have been conducted with air velocity 0.5 m/s, 1.26 m/s (base case), 2 m/s and 3 m/s. Fig. 5 shows the DPM concentration contours in the mine gallery when the intake air velocity is 0.5 m/s. The results show that high DPM concentration of over 200 µg/m³ is observed in almost the entire roadway. High DPM concentration also occurred on the passenger side of the vehicle. Downstream of the vehicle, high DPM concentration spreads across almost the entire cross-section of the roadway.

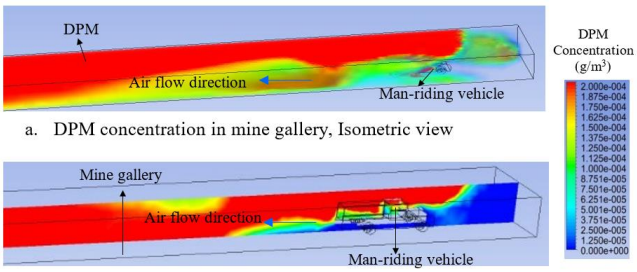

a. DPM concentration in mine gallery, Isometric view

b. DPM concentration in the vertical plane of symmetry of the gallery, Isometric view

Fig. 5. DPM distribution with 0.5 m/s air velocity.

Fig. 6 shows the DPM concentration contours for an intake air velocity of 2 m/s. High DPM concentration, near the smoke pipe, means that most of the particles dissipate towards the gallery ceiling due to high air velocity. At the middle of the roadway, negligible DPM concentration was observed up to 5 m downstream from the side of the vehicle. From 5 m to 10 m, high concentration is found near the roof. At locations further downstream, the DPM spreads throughout the entire roadway.

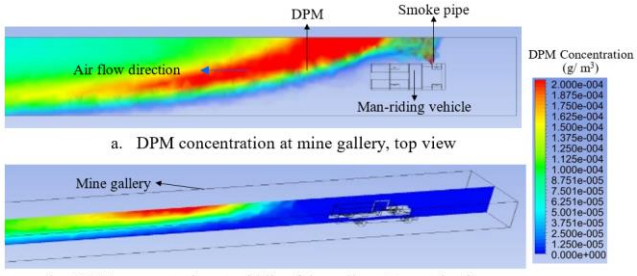

a. DPM concentration at mine gallery, top view

b. DPM concentration at middle of the gallery, Isometric view

Fig. 6. DPM distribution with 2 m/s air velocity, top view and center section view of mine gallery.

Fig. 7 shows the DPM concentration field corresponding to an intake air velocity is 3 m/s. The DPM flow is high at gallery roof. Negligible DPM concentration was observed at the middle of the roadway up to 20 m downstream of the vehicle. Beyond 20 m downstream of the vehicle, DPM concentration of 60 µg/m³ is observed near the ceiling and concentration reduced to zero towards the floor.

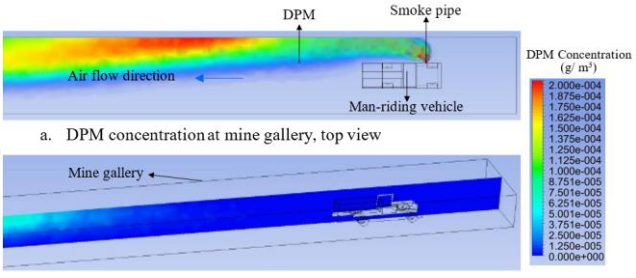

a. DPM concentration at mine gallery, top view

b. DPM concentration at middle of the gallery, Isometric view

Fig. 7. DPM distribution with 3 m/s air velocity, top and center section view of mine gallery.

Fig. 8 shows the DPM concentration with respect to different air velocities (0.5 m/s, 0.75 m/s, 1 m/s, 1.26 m/s, 2 m/s 2.5 m/s and 3 m/s) at various locations of sampling point 'a' (Fig. 1) downstream of the vehicle. If the intake air velocity is 0.5 m/s, the DPM concentration ranges from 250 µg/m³ to 289 µg/m³ over 15 m downstream of the vehicle. Further downstream, up to 40 m from the vehicle, the concentration spread is narrower, from about 220 µg/m³ to 258 µg/m³.

It is seen that beyond 15 m downstream of the vehicle, the DPM concentrations is uniform across the passage due to turbulent mixing, for all the different air velocities tested. The DPM concentration gradually reduces with increasing air velocity. For an air velocity of 0.5 m/s, the average DPM concentration downstream of the vehicle is about 249 µg/m³. For an air velocity of 3 m/s, the average DPM concentration is reduced to about 71 µg/m³.

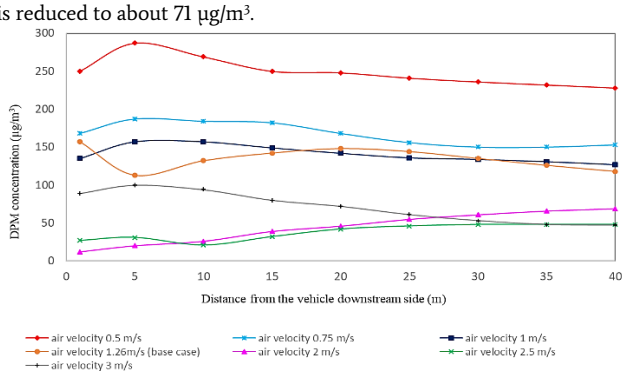

Fig. 8. DPM concentration with different air velocities at different sampling stations at sampling point 'a' with respect to DPM source.

Fig. 9 shows the DPM concentrations with respect to different air velocities (0.5 m/s, 0.75 m/s, 1 m/s, 1.26 m/s, 2 m/s, 2.5 m/s and 3 m/s) at various locations of sampling point 'b' (Fig. 1). If the air velocity is 0.5 m/s, from source to 40 m, high DPM concentration DPM evenly distributed between 220 µg/m³ to 234 µg/m³. If the air velocity is 3 m/s, negligible DPM concentration is observed in the middle of the airway up to about 15 m from the vehicle. Further downstream, the DPM concentration gradually increases to about 43 µg/m³ at 40 m. At the middle of the road way, from 1 m to 40 m the average DPM concentration is 226 µg/m³, 120 µg/m³, 66 µg/m³ and 19 µg/m³ for air velocities of with 0.5 m/s, 1 m/s, 2 m/s and 3 m/s respectively.

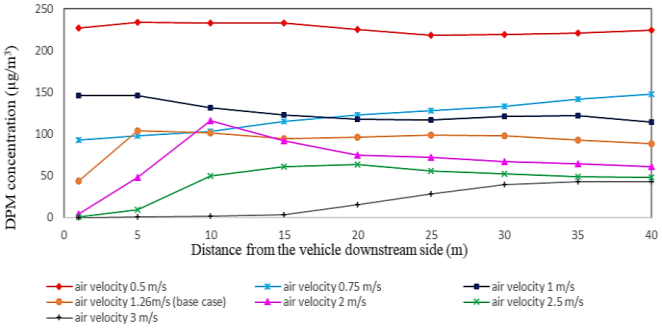

Fig. 9. DPM concentration with different air velocities at different sampling stations at sampling point 'b' with respect to DPM source.

Fig. 10 shows the DPM concentrations as a function of downstream distance with respect to different air velocities (0.5 m/s, 0.75 m/s, 1 m/s, 1.26 m/s, 2 m/s, 2.5 m/s and 3 m/s) at various locations of sampling point 'c' (Fig. 1). If the air velocity is 3 m/s, until 30 m no DPM concentration is observed at sample point 'c'. Further downstream, the DPM concentration gradually increases to 17 µg/m³ at 40 m. From 1 m to 40 m the average DPM concentration is about 213 µg/m³, 109 µg/m³, 28 µg/m³ and 3 µg/m³ for air velocities of 0.5 m/s, 1 m/s, 2 m/s and 3 m/s respectively.

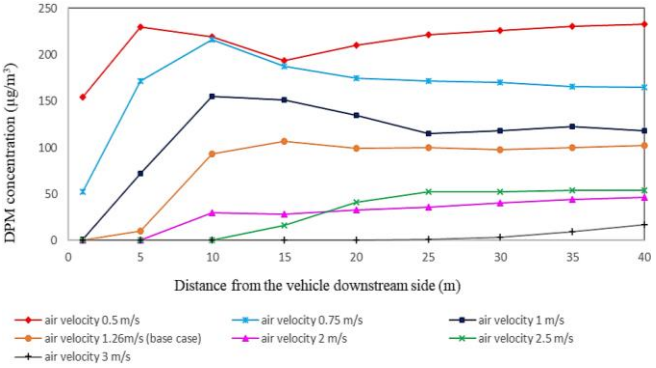

Fig. 10. DPM concentration with different air velocities at different sampling stations at sampling point 'c' with respect to DPM source.

Changes in the DPM concentration percentage with increasing intake

air velocities were calculated for different air velocities of 0.5 m/s, 0.75 m/s, 1 m/s, 1.26 m/s, 2 m/s, 2.5 m/s and 3 m/s at sampling point 'a', 'b' and 'c' at the sampling stations. Fig. 11 shows the details of DPM concentration changes at 10 m (a) and 40 m (b) downstream of the vehicle as functions of the intake air velocity.

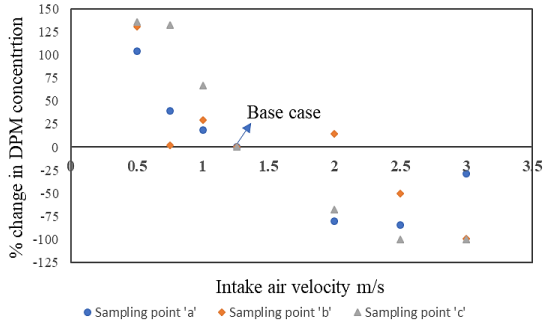

a. At 10 m downstream to the vehicle

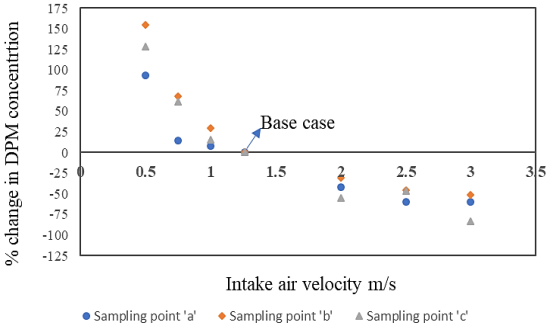

b. At 40 m downstream to the vehicle

Fig. 11. Changes in percentage of intake air velocity causes changes in DPM concentration percentages at 10 m and 40 m downstream to the vehicle.

At 10 m and 40 m downstream to the vehicle, the average DMP concentration variations of sample points 'a', 'b' and 'c' were calculated with different air velocities such as 0.5 m/s, 0.75 m/s, 1 m/s, 1.26 m/s, 2 m/s, 2.5 m/s and 3 m/s. Table 2 shows the details of average DPM concentration changes at 10 m and 40 m downstream of the vehicle with different intake air velocity.

Table 2. DPM concentration variations with air velocities at 10 m and 40 m downstream side.

Air velocity (m/s)	Air velocity Increased (+) / decreased (-)% from the base case	DPM concentration Increased (+) / decreased (-)% at 10 m downstream side	DPM concentration Increased (+) / decreased (-)% at 40 m downstream side
0.5	- 60%	+ 12%	+ 125%
0.7	- 40%	+ 57%	+ 48%
1	- 20%	+ 38%	+ 17%
1.26 (Base case)	0	0	0
2	+ 58%	- 44%	- 42%
2.5	+ 98%	- 78%	- 50%
3	+ 138%	- 75%	- 64%

6. Summary

CFD investigations were carried out to map contours of flow patterns of DPM generated by a man-riding vehicle operating in an underground coal mine and influenced by ventilation air flow. At 10 m downstream of the vehicle and at the middle of the roadway for air velocities of 0.5 m/s, 1 m/s, 2 m/s and 3 m/s, the DPM concentration is found to be 233 µg/m³, 131 µg/m³, 116 µg/m³ and 1 µg/m³ respectively. At 40 m downstream of the vehicle, if the velocity is reduced by 40% and 60% of the base case value (1.26 m/s), the average DPM concentration increased to 48% and 125% respectively. On the other hand, if the intake air velocity is increased by 58% and 98% of the base case value, the average DPM concentration decreased to 42% and 50% respectively. In summary, to minimise the health hazards due to the DPM, higher air velocities near diesel-operated vehicle working regions needs to be maintained. If the air velocity is low, miners will exposure to the high concentration DPM near downstream side of the vehicle.

Acknowledgments

The authors sincerely thank M/s Coal India Limited, DGMS, Govt. of India and IIT (ISM) Dhanbad for providing the necessary resources and extending cooperation during the field experiments.

REFERENCES

[1] Aleksandar B, Samuel J, Emanuele G C, James D N and Steven E M (2012). Controlling exposure to Diesel emissions in underground mines, Society for Mining Metallurgy and Exploration (SME).

[2] Bartlett C J S, Betts W E, Booth M, Giavazzi F, Guttmann H, Heinze P, Mayers R F, and Roberts D (1992). The chemical compassion of diesel particulate emissions, 92/51, Concawe.

[3] CMHS (Coal Mine Health and Safety Regulations) (2006). New South Wales.

[4] AIOH (Australian Institute of Occupational Hygienists) (2013). Diesel particulate matter and occupational health issues.

[5] MDG 29 (Mine Design Guideline 29) (2008). Guideline for the management of diesel engine pollutants in underground environments. Produced by Mine Safety Operations Division, New South Wales Department of Primary Industries. Retrieved January 5, 2018 from: http://www.resourcesandenergy.nsw.gov.au/__data/assets/pdf_file/0011/419465/MDG-29.pdf

[6] Morla R, Karekal S, Godbole A, Bhattachargee R, Nasina B and Inumal S (2018). Fundamental understanding of diesel-operated man-riding vehicle DPM dispersion- A case study. Journal of sustainable mining, https://doi.org/10.1016/j.jsm.2018.04.004.

[7] Roger O McClellan (2016). Diesel emissions and lung cancer. An evolution of recent epidemiological evidence for quantitative risk assessment. Critique of Health Effects Institute special report 19.

[8] Silverman D, Samanic C, Lubin J, Blair E, Stewart P, Vermeulen R, Coble J, Rothman N, Schleiff, P, Travis W, Ziegler R, Wacholder S and Attfield M (2011). The Diesel exhaust in Miners Study, A Cohort Mortality Study with Emphasis on Lung Cancer, Oxford University press.

[9] USEPA (U.S Environmental Protection Agency) (2002). Automobile emissions an overview. Office of the mobile service.

[10] Zheng Y (2011). Diesel particulate matter dispersion analysis in underground metal/ non-metal mines using CFD, Missouri University of science and technology, Ph.D. thesis.

[11] Zheng Y and Tien J C (2008). DPM dispersion study using CFD for underground metal/non-metal mines. 12th North American Ventilation Symposium.

[12] Zhen Y, Lan Hai, Mgesh T and Tien J (2011). DPM dispersion experiment at MST's experimental mine and comparison with CFD simulation. Journal of Coal science and Engineering, September.

[13] Zheng Y, Magesh T, Lan and Tien (2015). Simulation of DPM distribution in a long single entry with buoyancy effect. International Journal of mining science and technology. Vol.25, Issue 1, January 15.

[14] Zheng Y, Thiruvengadam Magesh, Lan Hai and Ten C Jerry (2015). Effect of auxiliary ventilations on diesel particulate matter

dispersion inside a dead-end entry, International journal of mining science and technology. Vol.25, Issue 6, November 15.

[15] Morla R, & karekal S (2017). Diesel Particulate Matter Investigations in Underground Coal Mines. International Journal of Engineering and Technology, 9(4): 2698–2703. http://www.enggjournals.com/ijet/abstract.html?file=17-09-04-401.

[16] Khan U M (2017). Real-time diesel particulate matter monitoring in underground mine atmospheres, association with the standard method and related challenges. Doctoral Dissertation. Missouri University of Science and Technology. Retrieved November 01, 2017, from: http://scholarsmine.mst.edu/doctoral_dissertations/2625/.

[17] Work Health and Safety (Mines and Petroleum Sites) Regulations 2014. Available from: https://www.legislation.nsw.gov.au/inforce/500011c6-2a99-440f-8799-8cbf39393930/2014-799.pdf. [accessed:2018-12-17].

[18] Work Health and Safety (Mines and Petroleum Sites) Act 2013. Available from: https://www.legislation.nsw.gov.au/inforce/2452de08-45ac-4954-856f-af17f88c9fc3/2013-54.pdf. [accessed:2018-12-09].

[19] Attfield M D, Schleiff P L, Lubin J H, Blair A, Stewart P A, Vermeulen R, Coble J B and Silverman D T (2012). The Diesel exhaust in Miners Study: A Cohort Mortality Study with Emphasis on Lung Cancer. Journal of the National Cancer Institute, 104(11), 869–883.doi: 10.1093/jnci/djs035.

[20] Silverman D, Samanic C, Lubin J, Blair E, Stewart P, Vermeulen R, Coble J, Rothman N, Schleiff P, Travis W, Ziegler R, Wacholder S and Attfield M (2011). The Diesel exhaust in Miners Study: A Cohort Mortality Study with Emphasis on Lung Cancer, Oxford University press. Available from: https://www.ncbi.nlm.nih.gov/pmc/articles/PMC3369553/pdf/djs034.pdf. [accessed:2018-12-18].

[21] Cox A, Costle D, King S, Huang A, Stewart R, Kennedy D and White Robert (1999). Diesel Emissions and Lung Cancer. Epidemiology and Quantitative Risk Assessment. Health Effect Institute. Available from: https://www.healtheffects.org/system/files/DieselEpi.pdf. [accessed:2018-12-09].